



HAL
open science

Oestrogen signalling inhibits invasive phenotype by repressing RelB and its target BCL2.

Xiaobo Wang, Karine Belguise, Nathalie Kersual, Kathrin H. Kirsch, Nora D. Mineva, Florence Galtier, Dany Chalbos, Gail E. Sonenshein

► To cite this version:

Xiaobo Wang, Karine Belguise, Nathalie Kersual, Kathrin H. Kirsch, Nora D. Mineva, et al.. Oestrogen signalling inhibits invasive phenotype by repressing RelB and its target BCL2.. *Nature Cell Biology*, 2007, 9 (4), pp.470-8. 10.1038/ncb1559 . inserm-00145547

HAL Id: inserm-00145547

<https://inserm.hal.science/inserm-00145547>

Submitted on 15 Oct 2007

HAL is a multi-disciplinary open access archive for the deposit and dissemination of scientific research documents, whether they are published or not. The documents may come from teaching and research institutions in France or abroad, or from public or private research centers.

L'archive ouverte pluridisciplinaire **HAL**, est destinée au dépôt et à la diffusion de documents scientifiques de niveau recherche, publiés ou non, émanant des établissements d'enseignement et de recherche français ou étrangers, des laboratoires publics ou privés.

Oestrogen signaling inhibits invasive phenotype by repressing RelB and its target *BCL2*

Xiaobo Wang¹, Karine Belguise¹, Nathalie Kersual³, Kathrin H. Kirsch¹, Nora D. Mineva², Florence Galtier³, Dany Chalbos³, and Gail E. Sonenshein^{1,4}

¹ Departments of Biochemistry, and ²Pathology and Laboratory Medicine and the Women's Health Interdisciplinary Research Center, Boston University School of Medicine, Boston, Massachusetts 02118, USA.

³ Inserm, U540, Montpellier, F-34090 and Univ. Montpellier I, Montpellier, F-34000, France.

⁴ Correspondence should be addressed to G.E.S. (email: gsonensh@bu.edu)

Aberrant constitutive expression of c-Rel, p65 and p50 NF- κ B subunits has been reported in over 90% of breast cancers^{1,2}. Recently, we characterized a *de novo* RelB NF- κ B subunit synthesis pathway, induced by the cytomegalovirus (CMV) IE1 protein, in which binding of p50/p65 NF- κ B and c-Jun/Fra-2 AP-1 complexes to the *RELB* promoter work in synergy to potently activate transcription³. While RelB complexes were observed in mouse mammary tumors induced by either ectopic c-Rel expression⁴ or carcinogen exposure⁵, little is known about RelB in human breast disease. Here, we demonstrate constitutive *de novo* RelB synthesis is selectively active in invasive estrogen receptor (ER) α negative breast cancer cells. ER α signaling reduced levels of functional NF- κ B and Fra-2 AP-1 and inhibited *de novo* RelB synthesis, leading to an inverse correlation between *RELB* and ER α

gene expression in human breast cancer tissues and cell lines. Induction of Bcl-2 by RelB promoted the more invasive phenotype of ER α negative cancer cells. Thus, inhibition of *de novo* RelB synthesis represents a new mechanism whereby ER α controls epithelial to mesenchymal transition (EMT).

To begin to assess the involvement of RelB in breast cancer, we selected the ZR-75, MCF-7, and T47D ER α positive, and Hs578T and MDA-MB-231 ER α negative human breast cancer cells, and the low expresser NF639 mouse mammary tumor line. Immunoblot analysis of whole cell protein extracts (WCEs) confirmed the expected profile of ER α (Fig. 1a, upper panel). Abundant levels of RelB protein were seen in Hs578T and MDA-MB-231 cells, while RelB was extremely low in ZR-75, MCF-7 and T47D cells; NF639 cells had an intermediate level (Fig. 1a, upper panel). Total levels of RelB and ER α proteins were found to display an inverse relationship (Fig. 1b). The difference in RelB expression in the cell lines was even more striking when the nuclear compartment was examined (Fig. 1a and b, lower panels).

Levels of *RELB* mRNA were also much higher in ER α negative vs positive breast cancer cells (Fig. 1c). To test whether an inverse correlation similarly exists in primary human breast cancers, a microarray gene expression dataset obtained from 295 patients⁶ and publicly available at Oncomine.org was analyzed. The levels of *RELB* mRNA were significantly higher in ER α negative vs ER α positive breast cancers (Fig. 1d) (p-value = 3.9×10^{-11} by Student t-test), consistent with the cell line data. Analysis of microarray datasets from three other studies confirmed this inverse correlation, including one⁷ with similar numbers of patient samples (p-value is 2.7×10^{-7}). Thus, *RELB* mRNA levels correlate inversely with ER α status in primary human breast cancers.

HAL author manuscript inserm-00145547, version 1

In *de novo* RelB synthesis mediated by the CMV IE1 protein, induction of binding of active c-Jun/Fra-2 AP-1 and p50/p65 NF- κ B complexes to one distal AP-1 and two proximal κ B elements, respectively, was shown to synergistically activate the *RELB* promoter in NIH 3T3 and smooth muscle cells³; whereas, c-Jun/c-Fos AP-1 was inactive. EMSA showed that ER α negative or low cells displayed much higher basal levels of AP-1 and NF- κ B binding compared to the ER α positive lines, as previously reported^{1,8} (Fig. 1e). Immunoblot analysis detected higher nuclear levels of Fra-2, c-Jun, and Fra-1 in ER α negative or low vs ER α positive cells; whereas JunB, and to a lesser extent JunD and c-Fos, were elevated in ER α positive cells (Fig. 1f).

To test for *de novo* RelB synthesis, transfection analysis was performed with the *RELB* promoter and vectors expressing various AP-1 subunits in Hs578T cells, which display constitutive p50/p65 NF- κ B activity⁹. Ectopic expression of c-Jun or Fra-2 alone led to an approximate 6- or 3-fold activation of *RELB* promoter, respectively (Fig. 2a), while the combination induced *RELB* promoter activity by ~26-fold (Fig. 2a). Similar synergy was seen in MDA-MB-231 and NF639 cells, whereas only an additive effect on *RELB* promoter activity was seen in the three ER α positive cells (Fig. 2b). Expression of c-Fos alone or in combination with c-Jun was unable to substantially induce *RELB* promoter activity. Somewhat surprisingly Fra-1, which was moderately active in NIH 3T3 cells³, failed to induce *RELB* promoter activity (Fig. 2a).

To test whether the synergy seen was indeed due to the high endogenous NF- κ B activity in ER α negative cells, the NF- κ B inhibitory protein I κ B- α was co-expressed in Hs578T and MCF-7 cells. I κ B- α expression strongly blocked the synergy between c-Jun and Fra-2 in Hs578T cells, while having little effect in MCF-7 cells or on c-Jun and Fra-2 alone (Fig. 2c).

When a *RELB* promoter construct with mutation of the κ B elements was analyzed, the co-expression of c-Jun and Fra-2 led to activation that was only additive in ER α negative cells (Fig. 2d), confirming the role of NF- κ B in the observed synergy.

To test directly the roles of c-Jun and Fra-2 in MDA-MB-231 and Hs578T cells, si-*JUN* or si-*FRA2* was used, which successfully reduced endogenous c-Jun and Fra-2 levels when added alone or in combination (Fig. 2e). Knockdown of c-Jun alone had little effect on RelB expression in MDA-MB-231, but substantially decreased RelB levels in Hs578T cells. An ~30-40% reduction in RelB levels was seen in both lines upon knockdown of Fra-2 alone. When both AP-1 subunits were reduced, an ~50-90% decrease in RelB levels occurred (Fig. 2e), confirming the role of c-Jun/Fra-2 heterodimers in activation of endogenous RelB. Lastly, the ability of c-Jun/Fra-2 and p50/p65 to act in synergy was tested directly using reduced suboptimal doses of each expression vector. A potent induction of the *RELB* promoter activity was observed in both ER α negative and positive cells (Fig. 2f). In contrast, Fra-2 and JunB, which are highly expressed in ER α positive cells, were unable to induce *RELB* promoter activity (data not shown). Thus, c-Jun/Fra-2 AP-1 and p50/p65 NF- κ B complexes, which are highly expressed in ER α negative or ER α low breast cancer cells, work in synergy to induce *de novo* RelB synthesis.

To assess the role of ER α in *de novo* RelB synthesis, MCF-7 and T47D cells were treated with the anti-estrogen ICI 182,780, which inhibits estrogen-dependent ER α function¹⁰ and decreases ER α protein levels¹¹ (Fig. 3a). ICI 182,780 treatment increased RelB protein and RNA levels (Fig. 3a), and induced both NF- κ B and AP-1 DNA binding and activity (Figs. 3b, 3c, Supplementary Information, Fig. S1a1-a4). Similarly, siRNA-induced knockdown of ER α substantially increased RelB levels in MCF-7 cells (Fig. 3d).

The effects of ectopic ER α expression were assessed in MDA-MB-231 and Hs578T cells in the presence of 17 β -estradiol (E2). Activation of ER α signaling substantially decreased RelB protein levels in MDA-MB-231 (61.8%) and Hs578T (47.4%) cells (Fig. 3e). To test the effects of active ER α on *de novo* RelB synthesis, *RELB* promoter constructs were used in MDA-MB-231 cells. Mutation of either the κ B or AP-1 site partially reduced basal promoter activity, and the double mutation resulted in an ~90% reduction, confirming the roles of the two factors in control of *RELB* promoter transcription. Ectopic ER α signaling resulted in strong repression of the WT *RELB* promoter, but only partial or no inhibition of the promoters with mutations in either the κ B or AP-1 site, or with a double mutation, respectively was seen (Fig. 3f). Thus, ER α signaling effectively represses *RELB* promoter activity driven by NF- κ B and AP-1.

While the mechanisms mediating repression of NF- κ B by ER α have been extensively studied¹², little is known about how ER α represses AP-1. We noted that ER α negative cells have higher levels of Fra-2 compared to positive ones, which led us to hypothesize that ER α signaling represses Fra-2 expression, and thereby AP-1 activity. Consistent with this hypothesis, inhibition of ER α in MCF-7 cells led to an increase in Fra-2 levels, while c-Jun was unaffected (Fig. 3g). Conversely, ectopic ER α signaling in MDA-MB-231 or Hs578T cells decreased Fra-2 expression (Fig. 3h). Knockdown of ER α in MCF-7 cells led to an increase in Fra-2 at day 1, which preceded the increase in RelB levels that were noted after 2 days (Fig. 3i). Similarly, induction of ER α signaling in MDA-MB-231 decreased Fra-2 levels after 1 day, preceding the decrease in RelB levels detectable after day 2 (Fig. 3j). Thus, repression of Fra-2 by ER α plays a substantial role in inhibition of *de novo* RelB synthesis.

Highly invasive and metastatic breast cancers are frequently ER α negative¹³⁻¹⁵. To test the role of RelB in invasive phenotype, Hs578T cells with knockdown of RelB (Hs578T/si-*RELB*) or control sense RelB cells (Hs578T/si-Control) were prepared (Fig. 4). Expression of Snail, the repressor of *E-cadherin* gene (*CDH1*) transcription, was decreased in Hs578T/si-*RELB* cells at both the mRNA and protein level (Figs. 4a, 4b). Furthermore, levels of the epithelial markers E-cadherin and γ -catenin were increased in Hs578T/si-*RELB* cells (Fig. 4b). A substantial decrease in fibronectin protein expression, a mesenchymal marker, was also observed. Importantly, Hs578T/si-*RELB* cells displayed decreased motility (Fig. 4c), and ability to form invasive colonies in Matrigel (Fig. 4d). Thus, RelB expression is required for maintenance of mesenchymal phenotype of ER α negative Hs578T breast cancer cells.

To determine whether ectopic expression of RelB can promote a more mesenchymal phenotype in ER α positive breast cancer cells, MCF-7 were transfected with pcDNA3-RELB expression vector or parental pcDNA3 EV DNA (MCF-7/RELB and MCF-7/EV, respectively), and several independent stable clones (MCF-7/RELB) expressing elevated RelB levels isolated (Fig. 4e-h). RelB overexpression was sufficient to lead to a marked decrease in E-cadherin levels (Fig. 4e, and see immunofluorescence in Supplementary Information, Fig. S3). RelB also increased levels of fibronectin, and vimentin, another mesenchymal marker (Fig. 4e). Stable RelB overexpression resulted in a more than 5-fold increase in migration of MCF-7 cells (Fig. 4f), enhanced cell scattering (Fig. 4g), and increased invasion through Matrigel [1.7-fold; 0.43 ± 0.08 vs 0.25 ± 0.06]. RelB overexpression also led to increased colony size in Matrigel (Fig. 4h); although, it was insufficient to allow for branching colony formation. Lastly, induction of RelB led to a more invasive gene profile within 48 h (Fig. 4i), and to a 4.7-fold increase in

migration (not shown). Thus, RelB expression in ER α positive breast cancer cells decreases epithelial and increases mesenchymal characteristics.

To further monitor the oncogenic effects of RelB expression, cells were subjected to irradiation and RelB was found to greatly promote resistance to killing (X.W., K.B., H. Ying, Z.X. Xiao, G.E.S., manuscript in preparation). This led us to examine the effects of RelB on expression of the pro-survival Bcl-2 protein, product of an NF- κ B p50/RelA target gene¹⁶. Inhibition of RelB led to a decrease in Bcl-2 protein levels in Hs578T cells, while ectopic RelB induced its expression in MCF-7 cells (Fig. 5a, upper panels). Consistently, endogenous Bcl-2 levels were higher in the ER α negative Hs578T and MDA-MB-231 lines compared to ER α positive ZR-75 and MCF-7 cells (Fig. 5b). To begin to test for transcriptional activation of the *BCL2* gene by RelB, we first confirmed that RelB levels controlled *BCL2* mRNA expression (Fig. 5a, lower panels). The *BCL2* gene has a TATA-less major P1 promoter, responsible for 95% of *BCL2* gene transcription, and a minor P2 promoter²⁰. In Hs578T cells, co-transfection of the WT *BCL2* P1 reporter construct with the si-*RELB* vector, led to an ~5-fold decrease in its activity compared to the sense control (Fig. 5c). Furthermore, the activity of the WT *BCL2* P1 promoter was potently induced upon co-transfection of vectors expressing RelB and p52 in either Hs578T cells (Fig 5d) or ZR-75 cells (see Supplementary Information, Fig. S2c). Induction of P1 promoter activity by NF- κ B in B cells has been shown to be mediated indirectly via protein-protein interaction with CREB, which is bound to a cyclic AMP response element (CRE) at bp –1535 to –1552¹⁷. When the CRE mutant and WT constructs were compared, the activity of the mutant *BCL2* construct in Hs578T cells expressing the si-control vector was significantly lower (Fig. 5c), and was unable to be substantially activated upon ectopic expression of RelB/p52 in

either Hs578T cells (Fig 5d) or ZR-75 cells (see Supplementary Information, Fig. S2c). Thus, RelB regulates *BCL2* promoter activity in breast cancer cells.

Recent evidence has correlated enhanced Bcl-2 levels with progression to a metastatic phenotype in prostate cancer¹⁸, leading us to hypothesize Bcl-2 mediates the effects of RelB. Ectopic Bcl-2 expression in MCF-7 and ZR-75 cells substantially decreased expression of E-cadherin and γ -catenin, while levels of the upstream regulator RelB were unaffected; migration of MCF-7 cells was enhanced (Figs. 5e, 5f). We then tested the ability of ectopic Bcl-2 to reverse the effects of inhibition of RelB in Hs578T cells. Ectopic Bcl-2 decreased expression of E-cadherin and γ -catenin, and essentially restored the ability of Hs578T/si-*RELB* cells to migrate and to form colonies with invasive phenotype in Matrigel (Fig. 5g-i). Lastly, knockdown of Bcl-2 decreased the ability of the Hs578T cells to form invasive colonies and to migrate (Fig. 5j-k), in association with increased E-cadherin and γ -catenin (Fig. 5l). Together, the data argue that Bcl-2 is a critical mediator of invasive properties induced by RelB.

Here, we show the ability of ER α to reduce AP-1 and NF- κ B binding and activity, and thereby to suppress *de novo* RelB synthesis, which represents a new mechanism whereby receptor signaling maintains a more epithelial phenotype. The effects on AP-1 were mediated, in large measure, via inhibition of Fra-2. Thus, transcriptional regulatory mechanisms control RelB NF- κ B activation and function. While early reports of RelB function implicated this subunit in mediating signals in the adaptive immune response¹⁹, recent studies have provided evidence for a role of RelB in cancer. We noted that several mammary tumors in MMTV-*c-Rel* transgenic mice expressed elevated nuclear levels of RelB⁴, and p52/RelB complexes were induced in mouse mammary tumors following carcinogen treatment⁵. p50/RelB was observed in mucosa-associated lymphoid tissue lymphomas, and these complexes inhibited apoptosis induced upon DNA

damage²⁰. RelB was the most frequently detected NF- κ B subunit in the nuclei of prostate cancer tissue, correlated directly with Gleason score²¹, and played a radioprotective role in aggressive prostate cancer cells²². In the present study, higher levels of RelB seen in ER α negative breast cancer cell lines and human breast cancers suggest an important role for RelB in advanced breast carcinomas. Consistent with our observations, RelB was recently implicated in inflammatory breast disease²³.

Huber and coworkers reported that NF- κ B activity was essential for the induction and maintenance of EMT and metastasis of *Ras*-transformed epithelial breast cells by TGF- β 1²⁴. We demonstrated that elevated NF- κ B activity is critical for maintenance of EMT in a c-Rel-driven mammary tumor cell line following carcinogen treatment²⁵. For the first time, we elucidate a critical role of RelB in EMT in breast cancer cells, and identify Bcl-2 as an important downstream mediator. RelB/p52 complexes were shown to induce *BCL2* P1 promoter activity. Protection from apoptosis by such genes as *BCL2* has recently been proposed to play an important role in promoting metastasis¹⁸. For example, ectopic expression of Bcl-2 in breast cancer cells increased their ability to metastasize to the lung²⁶. Our data indicate a role for Bcl-2 in negative regulation of epithelial markers. Interestingly, Bcl-2 has recently been shown to promote the degradation of I κ B- α and thereby induce NF- κ B activity in cardiac myocytes²⁷. This suggests a feed-forward mechanism, i.e., induction of Bcl-2 further enhances NF- κ B activity, which promotes a mesenchymal phenotype. Experiments are in progress to test this model in breast cancer cells. ER α was previously shown to inhibit EMT via its control of MTA3 levels and repression of *SNAIL* gene transcription²⁸. Our findings indicate inhibition of *de novo* RelB synthesis represents an additional mechanism by which ER α can control EMT, which provides a unifying model for the observed involvement of NF- κ B and AP-1 activities in EMT. Future

studies exploring the role of RelB as a biomarker or in therapeutic approaches for treatment of metastatic breast disease are warranted.

METHODS

Cell culture and treatment conditions. The NF639 cell line was derived from a mammary gland tumor in an mammary tumor virus (MMTV)-*ERBB2* transgenic mouse and cultured as described²⁹. ER α positive MCF-7, T47D and ZR-75 cells, and ER α negative Hs578T and MDA-MB-231 cells were purchased from the American Type Culture Collection (ATCC, Manassas, VA) and maintained in standard culturing medium as recommended by ATCC. Cultures were stripped of endogenous steroids by successive passages in phenol red free medium containing 10% dextran-coated charcoal (DCC)-stripped fetal bovine serum (FBS) (DCC-FBS) (2 days), and then 3% DCC-FBS (3 days)³⁰. MCF-7 cell lines containing pcDNA3 or pcDNA3-RELB and Hs578T cell lines containing human *pRELB*-siRNA or control *pRELB* sense (si-Control) were established as described⁵ and grown in the presence of 400 $\mu\text{g ml}^{-1}$ G418 (Sigma, St. Louis, MO) or 1 $\mu\text{g ml}^{-1}$ puromycin (Sigma), respectively. MCF-7 and Hs578T/si-*RELB* cell lines containing pBABE and pBABE-Bcl-2 were established by retroviral infection, as described³¹, and used 24 h post infection. Hs578T cells carrying pSM2c-sh-*BCL2* (V2HS_111806, Open Biosystems) or scrambled control were established by retroviral infection, as above. MCF-7 cells containing inducible C4_{bsr}R(TO) or C4_{bsr}R(TO-RelB) were established as described³². Expression of RelB was induced by treatment with 1 $\mu\text{g/ml}$ doxycycline for 48 h and analyzed as described. Where indicated, cells were treated with 1 μM ICI 182,780 or equivalent volume of vehicle ethanol (Tocris Cookson, Ellisville, MO). E2 was purchased from Sigma.

Plasmids and transfection analysis. The human 1.7 kB *RELB* promoter driving a luciferase reporter in pGL3 basic vector (p1.7 *RELB* promoter-Luc) and the pcDNA3-*RELB* construct containing human *RELB* cDNA sequence in the pcDNA3 expression vector were as described previously³. The pC4_{bsr}R(TO-RelB) construct was generated by subcloning the *Relb* cDNA into the Eco RI restriction site of the doxycycline inducible pC4_{bsr}R(TO) retroviral vector. The p1.7 *RELB* promoter-Luc vectors containing either wild type (WT), or mutant NF-κB (κB-Mut), or AP-1 (AP1-Mut) elements alone or with the double mutation (DM) were as prepared previously³. The thymidine kinase promoter-driven luciferase reporter plasmid controlled by six reiterated κB sites, was kindly provided by G. Rawadi (Hoechst-Marion-Roussel, Romainville, France). The thymidine kinase promoter-driven chloramphenicol acetyl transferase (CAT) plasmid controlled by five copies of the TPA responsive elements (TRE), was as described previously³. The NF-κB p50 or p65 constructs in pMT2T expression vector were as reported³. The IκB-α construct containing IκB-α SS32/36AA mutant in pRC-β-actin expression vector, was as reported⁵. The c-Jun, c-Fos, Fra-1, and Fra-2 AP-1 family member constructs in the pCI expression vector were as reported³. p*RELB* sense and p*RELB*-siRNA containing control or si-*RELB* oligonucleotides in pSIREN-RetroQ vector, were described previously³³. The human full-length *BCL2* constructs in pcDNA3 or pBabe were as reported³⁴. The SV40 β-galactosidase (β-gal) reporter vector was as reported³. For transfection into six well and P100 plates, 3 or 10 μg total DNA was transfected, respectively. For transient transfection, cultures were incubated for 48 h in the presence of DNA and Fugene6 (Roche Diagnostics Co., Indianapolis, IN) or Geneporter2 (Gene Therapy System Inc., San Diego, CA) Transfection Reagent. All transient transfections were performed a minimum of three times, in triplicate. For stable transfection, cells were incubated for 48 h with DNA and GenePorter2 before adding 10 μg ml⁻¹ blasticidin, 400 μg ml⁻¹ G418, or 1 μg ml⁻¹

puromycin, as appropriate, for stable selection. CAT and luciferase assays were performed as described^{2,4}. Co-transfection of the SV40- β -gal expression vector was used to normalize for transfection efficiency, as described⁴. Sequences of *FRA2*, *JUN*, and GFP siRNA duplexes have been previously described³⁵. For the RelB repression studies, the *ER α* siRNA duplex (Dharmacon, Chicago, IL) targeted the following sequence: AAGATCCTGAAACAGAGCATG (sense strand). Transfections (100 nM final) were carried out using Oligofectamine (Invitrogen, Carlsbad, CA), in Optimem serum-free medium, 24 h after plating. When multiple transfections were performed, cells were re-plated 48 h after transfection (dilution 1:2). For kinetics studies, cell extracts were processed for immunoblotting 48 h after the last transfection. *ER α* validated StealthTM RNAi and Stealth RNAi negative controls from Invitrogen were used. Duplexes (0.9 nM final) were introduced in cells using Lipofectamine RNAiMAX reagent (Invitrogen) by reverse transfection according to the manufacturer's protocol. Similar results were obtained with the 2 different *ER α* duplexes. The *BCL2* P1 promoter constructs with WT or mutant CRE sites were as described¹⁷.

Immunoblot analysis, antibodies, and immunofluorescence. WCEs (total protein extracts) were prepared in RIPA buffer (10 mM Tris [pH 7.5], 150 mM NaCl, 10 mM EDTA, 1% NP-40, 0.1% SDS, 1% sodium sarcosyl, 0.2 mM phenylmethylsulfonylfluoride, 10 μ g ml⁻¹ leupeptin, 1 mM dithiothreitol). Nuclear extracts were prepared as previously described²⁹. Immunoblotting was performed as we have described²⁹. Antibodies against NF- κ B members: p65 (sc-372) and RelB (sc-226), or AP-1 members: JunB (sc-46), JunD (sc-74), c-Fos (sc-7202), Fra-1 (sc-183), Fra-2 (sc-604), Bcl-2 (sc-492), or against Snail (*Snai1*, sc-10432) or Lamin B (sc-6217), were purchased from Santa Cruz Biotechnology (Santa Cruz, CA). Antibodies against c-Jun and *ER α*

were purchased from Cell Signaling (Danvers, MA) and NeoMarker (Fremont, CA), respectively. The E-cadherin, fibronectin, and γ -catenin antibodies were purchased from BD Transduction Lab (Franklin Lakes, NJ), and the β -actin (AC-15) and cyclin D1 (Ab-3) antibodies were from Sigma and Oncogene (Boston, MA), respectively. Immunofluorescence was performed as we have published previously²⁵.

EMSA. Nuclear extracts were prepared and samples (5 μ g) subjected to binding and EMSA as described². The sequences of the oligonucleotide containing the consensus AP-1 element and NF- κ B element upstream of the *c-Myc* promoter are as follows:

AP-1, 5'-GATCCGCTTGATGACTCAGCCGGAAG-3';

NF- κ B, 5'-GATCCAAGTCCGGGTTTTCCCAACC-3'. The Oct-1 sequence is as reported previously².

RT-PCR and Northern blot analysis. RNA, isolated using Trizol reagent (Invitrogen), was quantified by measuring A_{260} . $A_{260}:A_{280}$ ratios were between 1.8 and 2. RNA samples were treated with RQ1 RNase-free DNase (Promega Corporation, Madison WI). For reverse transcriptase (RT)-PCR, 1 μ g RNA was reverse transcribed with Superscript RNase H-RT in the presence of 100 ng of random primers (Invitrogen). PCR for *SNAIL* was performed in a Thermal Cycler for 20 cycles as follows: 94°C for 30 sec, 55°C for 30 sec and 72°C for 30 sec, and for *BCL2* for 30 cycles as follows: 94°C for 30 sec, 60°C for 30 sec and 72°C for 45 sec. The primers specific for human *SNAIL* are as follows: sense (5'-GAAAGGCCTTCAACTGCAAA-3') and antisense (5'-TGACATCTGAGTGGGTCTGG-3'). The primers specific for human *BCL2* are: sense (5'-CATTTCACGTCAACAGAATTG-3') and antisense (5'-

AGCACAGGATTGGATATTCCAT-3'). As a loading control, PCR for *GAPDH* was performed in a Thermal Cycler for 15 cycles: 94°C for 30 sec, 55°C for 30 sec and 72°C for 30 sec. RNA samples (20 µg) were subjected to Northern blot analysis, as described³. The 2.1-kb Eco RI inserts of the human *RELB* or mouse *Relb* cDNA expression vectors were used as probes.

Matrigel outgrowth assays. Cells (2×10^4) were suspended at 4°C in Matrigel (0.2 ml, 6.3 mg ml⁻¹) (BD Biosciences, Bedford, MA), an extracellular matrix extracted from Engelbreth-Holm-Swarm mouse tumors, and added to a pre-set Matrigel layer in 24-well plates as described²⁵. The top Matrigel cell layers were covered with culture medium containing 10% FBS.

Migration and invasion assays. Suspensions of 1 to 2.5×10^5 MCF-7 or Hs578T cells were layered, in triplicate, in the upper compartments of a Transwell (Costar, Cambridge, MA) on an 8-mm diameter polycarbonate filter (8 µm pore size), and incubated at 37°C for the indicated times. All migration assays were performed two to three times, in triplicate. For invasion assays, filters were precoated with 60 µg of Matrigel. Migration of the cells to the lower side of the filter was evaluated with the acid phosphatase enzymatic assay using p-nitrophenyl phosphate and OD_{410nm} determination. The mean ± SD are presented. All invasion assays were performed two times, in triplicate.

Gene expression and statistical analysis. The Van de Vijver_Breast carcinoma microarray dataset (reporter number NM_006509⁶) was accessed using the ONCOMINETM Cancer Profiling Database (www.oncomine.org). The dataset includes 69 ER negative and 226 ER positive human primary breast carcinoma samples. Box plots, depicting the distribution of *RELB* expression

HAL author manuscript inserm-00145547, version 1

within each ER α group and a Student t-test giving a p-value for the comparison of *RELB* expression between the two ER α groups were obtained directly through the OncoPrint 3.0 software. The line within the box represents the median expression value for each group, and the upper and lower edges of the box indicate the 75th and 25th percentile of the distribution, respectively. The lines (whiskers) emerging from each box extend to the smallest and largest observations; the black dots outside the ends of the whiskers are outlier data points.

ACKNOWLEDGEMENTS

We thank Finn-Eirik Johansen, Carlos V. Paya, Stanley Korsmeyer, and Linda M. Boxer for cloned DNAs, T. Akagi for the inducible retroviral vector, and P. Leder for the NF639 cell line. These studies were supported by NIH grants ES11624 and CA36355.

REFERENCES

1. Nakshatri, H., Bhat-Nakshatri, P., Martin, D. A., Goulet, R. J., Jr. & Sledge, G. W., Jr. Constitutive activation of NF-kappaB during progression of breast cancer to hormone-independent growth. *Mol Cell Biol* **17**, 3629-39 (1997).
2. Sovak, M. A. et al. Aberrant nuclear factor-kappaB/Rel expression and the pathogenesis of breast cancer. *J Clin Invest* **100**, 2952-60 (1997).
3. Wang, X. & Sonenshein, G. E. Induction of the RelB NF-kappaB subunit by the cytomegalovirus IE1 protein is mediated via Jun kinase and c-Jun/Fra-2 AP-1 complexes. *J Virol* **79**, 95-105 (2005).
4. Romieu-Mourez, R. et al. Mouse mammary tumor virus c-rel transgenic mice develop mammary tumors. *Mol Cell Biol* **23**, 5738-54 (2003).
5. Demicco, E. G. et al. RelB/p52 NF-kappaB complexes rescue an early delay in mammary gland development in transgenic mice with targeted superrepressor IkappaB-alpha expression and promote carcinogenesis of the mammary gland. *Mol Cell Biol* **25**, 10136-47 (2005).
6. van de Vijver, M. J. et al. A gene-expression signature as a predictor of survival in breast cancer. *N Engl J Med* **347**, 1999-2009 (2002).
7. Wang, Y. et al. Gene-expression profiles to predict distant metastasis of lymph-node-negative primary breast cancer. *Lancet* **365**, 671-9 (2005).
8. Philips, A. et al. FRA-1 expression level modulates regulation of activator protein-1 activity by estradiol in breast cancer cells. *Mol Endocrinol* **12**, 973-85 (1998).
9. Romieu-Mourez, R. et al. Roles of IKK kinases and protein kinase CK2 in activation of nuclear factor-kappaB in breast cancer. *Cancer Res* **61**, 3810-8 (2001).
10. Hyder, S. M., Chiappetta, C., Murthy, L. & Stancel, G. M. Selective inhibition of estrogen-regulated gene expression in vivo by the pure antiestrogen ICI 182,780. *Cancer Res* **57**, 2547-9 (1997).
11. Oliveira, C. A. et al. The antiestrogen ICI 182,780 decreases the expression of estrogen receptor-alpha but has no effect on estrogen receptor-beta and androgen receptor in rat efferent ductules. *Reprod Biol Endocrinol* **1**, 75 (2003).
12. Kalaitzidis, D. & Gilmore, T. D. Transcription factor cross-talk: the estrogen receptor and NF-kappaB. *Trends Endocrinol Metab* **16**, 46-52 (2005).
13. Horwitz, K. B. Mechanisms of hormone resistance in breast cancer. *Breast Cancer Res Treat* **26**, 119-30 (1993).
14. Johnston, S. R. et al. Changes in estrogen receptor, progesterone receptor, and pS2 expression in tamoxifen-resistant human breast cancer. *Cancer Res* **55**, 3331-8 (1995).
15. Rochefort, H. et al. Estrogen receptor mediated inhibition of cancer cell invasion and motility: an overview. *J Steroid Biochem Mol Biol* **65**, 163-8 (1998).
16. Catz, S. D. & Johnson, J. L. Transcriptional regulation of bcl-2 by nuclear factor kappa B and its significance in prostate cancer. *Oncogene* **20**, 7342-51 (2001).
17. Xiang, H., Wang, J. & Boxer, L. M. Role of the Cyclic AMP Response Element in the bcl-2 Promoter in the Regulation of Endogenous Bcl-2 Expression and Apoptosis in Murine B Cells. *Mol Cell Biol* **26**, 8599-606 (2006).
18. Mehlen, P. & Puisieux, A. Metastasis: a question of life or death. *Nat Rev Cancer* **6**, 449-58 (2006).
19. Burkly, L. et al. Expression of relB is required for the development of thymic medulla and dendritic cells. *Nature* **373**, 531-6 (1995).

20. Stoffel, A., Chaurushiya, M., Singh, B. & Levine, A. J. Activation of NF-kappaB and inhibition of p53-mediated apoptosis by API2/mucosa-associated lymphoid tissue 1 fusions promote oncogenesis. *Proc Natl Acad Sci U S A* **101**, 9079-84 (2004).
21. Lessard, L., Begin, L. R., Gleave, M. E., Mes-Masson, A. M. & Saad, F. Nuclear localisation of nuclear factor-kappaB transcription factors in prostate cancer: an immunohistochemical study. *Br J Cancer* **93**, 1019-23 (2005).
22. Josson, S. et al. RelB regulates manganese superoxide dismutase gene and resistance to ionizing radiation of prostate cancer cells. *Oncogene* (2005).
23. Van Laere, S. J. et al. Nuclear factor-kappaB signature of inflammatory breast cancer by cDNA microarray validated by quantitative real-time reverse transcription-PCR, immunohistochemistry, and nuclear factor-kappaB DNA-binding. *Clin Cancer Res* **12**, 3249-56 (2006).
24. Huber, M. A. et al. NF-kappaB is essential for epithelial-mesenchymal transition and metastasis in a model of breast cancer progression. *J Clin Invest* **114**, 569-81 (2004).
25. Shin, S. R., Sanchez-Velar, N., Sherr, D. H. & Sonenshein, G. E. 7,12-dimethylbenz(a)anthracene treatment of a c-rel mouse mammary tumor cell line induces epithelial to mesenchymal transition via activation of nuclear factor-kappaB. *Cancer Res* **66**, 2570-5 (2006).
26. Schmitt, C. A. et al. Dissecting p53 tumor suppressor functions in vivo. *Cancer Cell* **1**, 289-98 (2002).
27. de Moissac, D., Mustapha, S., Greenberg, A. H. & Kirshenbaum, L. A. Bcl-2 activates the transcription factor NFkappaB through the degradation of the cytoplasmic inhibitor IkappaBalpha. *J Biol Chem* **273**, 23946-51 (1998).
28. Fujita, N. et al. MTA3, a Mi-2/NuRD complex subunit, regulates an invasive growth pathway in breast cancer. *Cell* **113**, 207-19 (2003).
29. Guo, S. & Sonenshein, G. E. Forkhead box transcription factor FOXO3a regulates estrogen receptor alpha expression and is repressed by the Her-2/neu/phosphatidylinositol 3-kinase/Akt signaling pathway. *Mol Cell Biol* **24**, 8681-90 (2004).
30. Philips, A., Chalbos, D. & Rochefort, H. Estradiol increases and anti-estrogens antagonize the growth factor-induced activator protein-1 activity in MCF7 breast cancer cells without affecting c-fos and c-jun synthesis. *J Biol Chem* **268**, 14103-8 (1993).
31. Romieu-Mourez, R., Landesman-Bollag, E., Seldin, D. C. & Sonenshein, G. E. Protein kinase CK2 promotes aberrant activation of nuclear factor-kappaB, transformed phenotype, and survival of breast cancer cells. *Cancer Res* **62**, 6770-8 (2002).
32. Min, C. et al. The tumor suppressor activity of the lysyl oxidase pro-peptide reverses invasive phenotype of Her-2/neu driven breast cancer. *Cancer Res* In press (2007).
33. Schjerven, H., Tran, T. N., Brandtzaeg, P. & Johansen, F. E. De novo synthesized RelB mediates TNF-induced up-regulation of the human polymeric Ig receptor. *J Immunol* **173**, 1849-57 (2004).
34. Sentman, C. L., Shutter, J. R., Hockenbery, D., Kanagawa, O. & Korsmeyer, S. J. bcl-2 inhibits multiple forms of apoptosis but not negative selection in thymocytes. *Cell* **67**, 879-88 (1991).
35. Freund, A. et al. Mechanisms underlying differential expression of interleukin-8 in breast cancer cells. *Oncogene* **23**, 6105-14 (2004).

FIGURE LEGENDS

Figure 1. RelB levels are inversely correlated with ER α status in breast cancer cells. (a) Upper panel. WCEs (25 μ g) from the indicated breast cancer cells were analyzed by immunoblotting with antibodies against ER α , RelB, and β -actin, which confirmed equal loading. Lower panel. Nuclear extracts (25 μ g) from the indicated breast cancer cells were analyzed by immunoblotting for ER α , RelB and Lamin B. MB-231, MDA-MB-231. (b) The blots for the human cell lines in (a) were scanned and the values for ER α and RelB normalized to β -actin (upper panel) or to Lamin B (lower panel) plotted as a percent of the values in ZR-75 and MDA-MB-231 cells, respectively (set at 100%), showing an inverse relationship between these two proteins. (c) Samples of mRNA (20 μ g) were subjected to Northern blot analysis using either human *RELB* (h) or mouse *Relb* (m) cDNA, as probe, as they only weakly hybridize across species. Ethidium bromide staining confirmed equal loading. In RT-PCR analysis, *RELB* mRNA levels in ZR-75, MCF-7, T47D, and Hs578T cells were 3.9%, 16.0%, 19.2%, and 57.2% of those seen in MDA-MB-231 cells (not shown). (d) Box plots of data from the Van de Vijver_Breast carcinoma microarray dataset (reporter number NM_006509⁶) was accessed using the ONCOMINETM Cancer Profiling Database (www.oncomine.org) and is plotted on a log scale. The dataset includes 69 ER α negative and 226 ER α positive human primary breast carcinoma samples. A Student t-test, performed directly through the Oncomine 3.0 software, showed the difference in *RELB* expression between the two groups was significant (p-value = 3.9 e-11). (e) Nuclear extracts (5 μ g) were subjected to EMSA binding of AP-1, NF- κ B, or Oct-1, which confirmed equal loading. The positions of the previously identified p50/p50 and p50/p65 NF- κ B complexes in Hs578T cells⁹ are as indicated. (f) Nuclear extracts (25 μ g) were analyzed

for Fra-2, c-Jun, Fra-1, c-Fos, JunB, JunD, or β -actin. Uncropped scans of the top two panels in **a** and **e** are shown in the Supplementary Information, Fig. S5a and S5b, respectively.

Figure 2. c-Jun/Fra-2 AP-1 and p50/p65 NF- κ B complexes synergistically induce *RELB* promoter activity in ER α negative breast cancer cells. (a) Hs578T cells were transiently transfected, in triplicate, with 0.5 μ g p1.7 *RELB* promoter-Luc vector, 0.5 μ g of the indicated AP-1 subunit expression vector, 0.5 μ g SV40- β -gal and empty vector (EV) pcDNA3 to make a total of 3.0 μ g DNA. Post-transfection (48 h), luciferase and β -gal activities were determined and normalized luciferase activities presented (mean \pm S.D. from three separate experiments). (b) The indicated breast cancer cell lines were transiently transfected with 1.0 μ g p1.7 *RELB* promoter-Luc vector, 0.5 μ g c-Jun and Fra-2 AP-1 subunit expression vector, 0.5 μ g SV40- β -gal and EV DNA to a 3.0 μ g DNA total, and analyzed as in (a). (c) Hs578T or MCF-7 cells were transiently transfected with 0.5 μ g p1.7 *RELB* promoter-Luc DNA, 0.5 μ g of the indicated AP-1 subunit expression vector, in the absence or presence of 0.5 μ g I κ B- α vector DNA, 0.5 μ g SV40- β -gal and EV DNA to a 3.0 μ g DNA total, and processed as above. (d) Hs578T cells were transiently transfected with 0.5 μ g of WT or κ B-mutant p1.7 *RELB* promoter-Luc vector, AP-1 subunit, SV40- β -gal and EV DNA and analyzed as in (a). (e) MDA-MB-231 or Hs578T cells were transfected with siRNA directed against *JUN* or *FRA2*, or against both genes. All duplexes were used at a concentration of 100 nM and 100 nM GFP siRNA was added when only one gene was targeted. Post-transfection (48 h), WCEs were analyzed by immunoblotting for RelB, c-Jun, Fra-2, and β -actin. (Please note loading for si-*JUN* and si-*FRA2* was reversed in the two blots.) The blots were scanned and the values for RelB, c-Jun, and Fra-2 normalized to β -actin. Values

relative to the control siRNA (set at 100%) are given below each lane, showing their corresponding levels of decrease. (f) The indicated breast cancer cell lines were transiently transfected with 0.5 μ g p1.7 *RELB* promoter-Luc vector, 0.25 μ g of the indicated AP-1 or NF- κ B subunit expression vectors, 0.5 μ g SV40- β -gal and EV DNA to a 3.0 μ g DNA total, and analyzed as in (a).

Figure 3. ER α represses NF- κ B and AP-1 activities and reduces RelB levels. (a-b) MCF-7 cells were treated with 1 μ M ICI 182,780 (ICI) or vehicle ethanol (Eth) for 48 h. (a) WCEs (25 μ g) were analyzed by immunoblotting (left panel). RNA was subjected to Northern blotting and ethidium bromide staining (right panel). (b) Nuclear extracts were subjected to EMSA, as in Fig. 1e. (c) MCF-7 cells were transiently transfected, in triplicate, with 0.5 μ g NF- κ B (κ B-Luc) or AP-1 (TRE-CAT) element driven constructs and 0.5 μ g SV40- β -gal. Post-transfection (6 h), cells were treated with ICI 182,780 or ethanol for 40 h. Normalized values are presented as the mean \pm S.D. from three experiments (control set to 1). (d) MCF-7 cells were transfected with si-*ER α* or GFP control siRNA. After 3 successive 48 h transfections, WCEs were analyzed by immunoblotting. (e) Cells, growing in medium depleted of steroids, were transfected with 10 μ g ER α expression vector or EV DNA for 6 h and then treated for 40 h with 10 nM E2. WCEs were analyzed by immunoblotting. (f) Cells in steroid-free medium were transfected, in triplicate, with 0.5 μ g of the indicated p1.7 *RELB* promoter-Luc vector, 1 μ g ER α expression vector or EV pcDNA3, 0.5 μ g SV40- β -gal, and EV DNA (3.0 μ g total). After 6 h, cells were treated for 40 h with 10 nM E2. Normalized data are presented relative to the WT reporter with EV DNA (mean \pm S.D from three experiments). (g) WCEs from MCF-7 cells, treated as in part a, were analyzed by immunoblotting. (h) MDA-MB-231 and Hs578T cells, transfected with an

ER α expression or EV DNA, were processed as in part e. **(i)** MCF-7 cells, transfected with si-ER α or control siRNA, were lysed after 1, 2 or 4 days and WCEs analysed. Values for RelB and Fra-2 normalized to β -actin relative to control (set at 100%) are presented below. **(j)** Stable MDA-MB-231 cells expressing ER α , cultivated in medium depleted of steroids, were treated with 10 nM E2 as indicated. Values for RelB and Fra-2 normalized to β -actin in WCEs, relative to control, are given.

Figure 4. RelB expression promotes mesenchymal phenotype of breast cancer cells. (a-d)

Stable Hs578T transfectants expressing either siRNA *RELB* (Hs578T/si-*RELB*) or sense *RELB* (Hs578T/si-Control) (si-Con) were prepared. Expression of si-*RELB* decreased levels of *RELB* mRNA and RelB protein in the nucleus, but had no effect on levels of the p65 NF- κ B subunit (see Supplementary Information, Figs. S1b1 and S1b2), consistent with findings of Johansen and coworkers³³. **(a)** RNA was analyzed by RT-PCR for levels of *SNAIL* and *GAPDH* RNA, as a control for equal loading. **(b)** WCEs (50 μ g) were analyzed by immunoblotting for E-cadherin, γ -catenin, Snail, fibronectin (FN), and β -actin. The effects of si-*RELB* on MDA-MB-231 cells were tested and similar data were obtained (see Supplementary Information, Fig. S1c). **(c)** Cells were subjected, in triplicate, to a migration assay for 4 h. Cells that migrated to the lower side of the filter quantified by spectrometric determination at OD_{410nm} (mean \pm S.D). Data presented are from one representative of 3 experiments. **(d)** Cells were subjected to Matrigel outgrowth analysis. After 5 days, the colonies were photographed (50x magnification). **(e-h)** Stable MCF-7 clones expressing either *RELB* or EV DNA were isolated: RELB(1), RELB(2), EV(1), and EV(2). Ectopic RelB expression increased NF- κ B reporter activity, and levels of cyclin D1, but failed to alter the levels of p65 (see Supplementary Information, Figs. S2a and S2b). **(e)** WCEs

were subjected to immunoblot analysis for E-cadherin (E-cad), fibronectin (FN), vimentin (Viment), and β -actin. While all of the clones showed an increase in fibronectin, the extent of the increase varied. (f) Clones were subjected to a migration assay, as in part (c) (mean \pm S.D from three separate experiments). (g) MCF-7 stable clones (1×10^4 cells ml^{-1}) were plated and after 2 days photographed (50x magnification). (h) Clones were subjected to Matrigel outgrowth analysis. After 15 days of growth, the colonies were photographed (50x magnification). (i) Stable MCF-7 cells with an inducible RelB expression vector were treated with 1 $\mu\text{g/ml}$ doxycycline. After 48 h, WCEs were subjected to immunoblot analysis for RelB, E-cadherin (E-cad), vimentin and β -actin, as above. Scale bar, 100 μm in parts d, g, and h. An uncropped scan of the E-cadherin panel in i is shown in the Supplementary Information, Fig. S5c.

Figure 5. Bcl-2 mediates control of invasive properties of breast cancer cells. (a) WCEs (25 μg) and RNA were prepared from Hs578T/si-*RELB* or Hs578T/si-Control and from MCF-7 cells expressing RELB (clone 1) or with EV DNA, and analyzed by immunoblotting (Upper panels), and RT-PCR (Lower panels). Similar data were obtained with other MCF-7 clones expressing RELB (not shown). (b) ZR-75, MCF-7, Hs578T and MDA-MB-231 WCEs (25 μg) were analyzed for Bcl-2 and β -actin. (c) Hs578T cells were transiently transfected with 0.5 μg WT or CRE-Mutant *BCL2* P1 promoter-Luc vector, 1.0 μg of the siRNA *RELB* expression or control sense vector (si-Con), 0.5 μg SV40- β -gal and EV pcDNA3 (3.0 μg DNA total) for 48 h. Normalized luciferase activities are presented (mean \pm S.D. from three separate experiments). (d) Hs578T cells were transiently transfected, in triplicate, with 1.0 μg WT or CRE-Mutant *BCL2* P1 promoter-Luc vector, the indicated dose of p52 and RelB expression vectors, 0.5 μg SV40- β -gal and EV pcDNA3 (3.5 μg DNA total), and analyzed as in (c). (e) WCEs (25 μg) were

prepared from MCF-7 and ZR-75 cells, ectopically expressing EV or full length Bcl-2, and analyzed for EMT gene expression, Bcl-2, and RelB, as above. Ectopic Bcl-2 also resulted in a substantial decrease in E-cadherin staining in MCF-7 cells (see Supplementary Information, Fig. S4) **(f)** Stable mixed populations of MCF-7 cells expressing Bcl-2 or EV DNA were subjected to a migration assay for 24 h, as in Fig 4c. **(g)** WCEs (50 μ g) were prepared from Hs578T/si-*RELB* cells, ectopically expressing full length Bcl-2, and analyzed, as above. **(h-i)** Hs578T/si-*RELB* cells were transiently infected with pBABE-Bcl-2 or EV pBABE DNA. After 24 h, cells were subjected to a migration assay for 4 h **(h)**, or Matrigel colony formation assay for 12 days **(i)**. **(j-l)** Hs578T cells were infected with pSM2c-sh-*BCL2* or scrambled control (Control). **(j)** Cells were subjected to Matrigel assay in the presence of 2 μ g/ml puromycin. **(k)** Stable mixed populations, isolated using puromycin selection, were subjected to a migration assay for 4 h. **(l)** WCEs (25 μ g) were assessed by immunoblotting. Scale bar, 100 μ m in parts i and j.

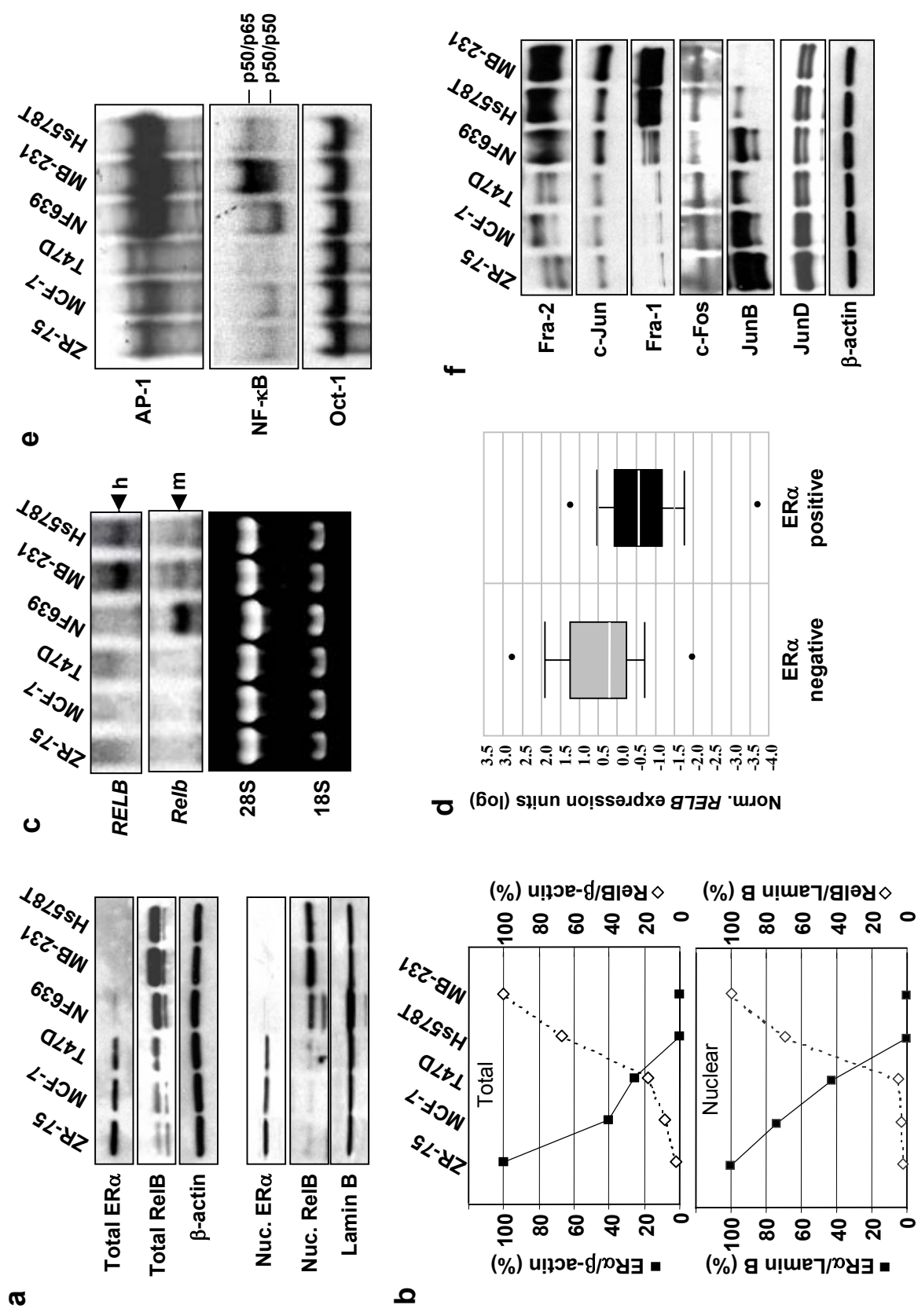


Fig. 1, Wang et.al

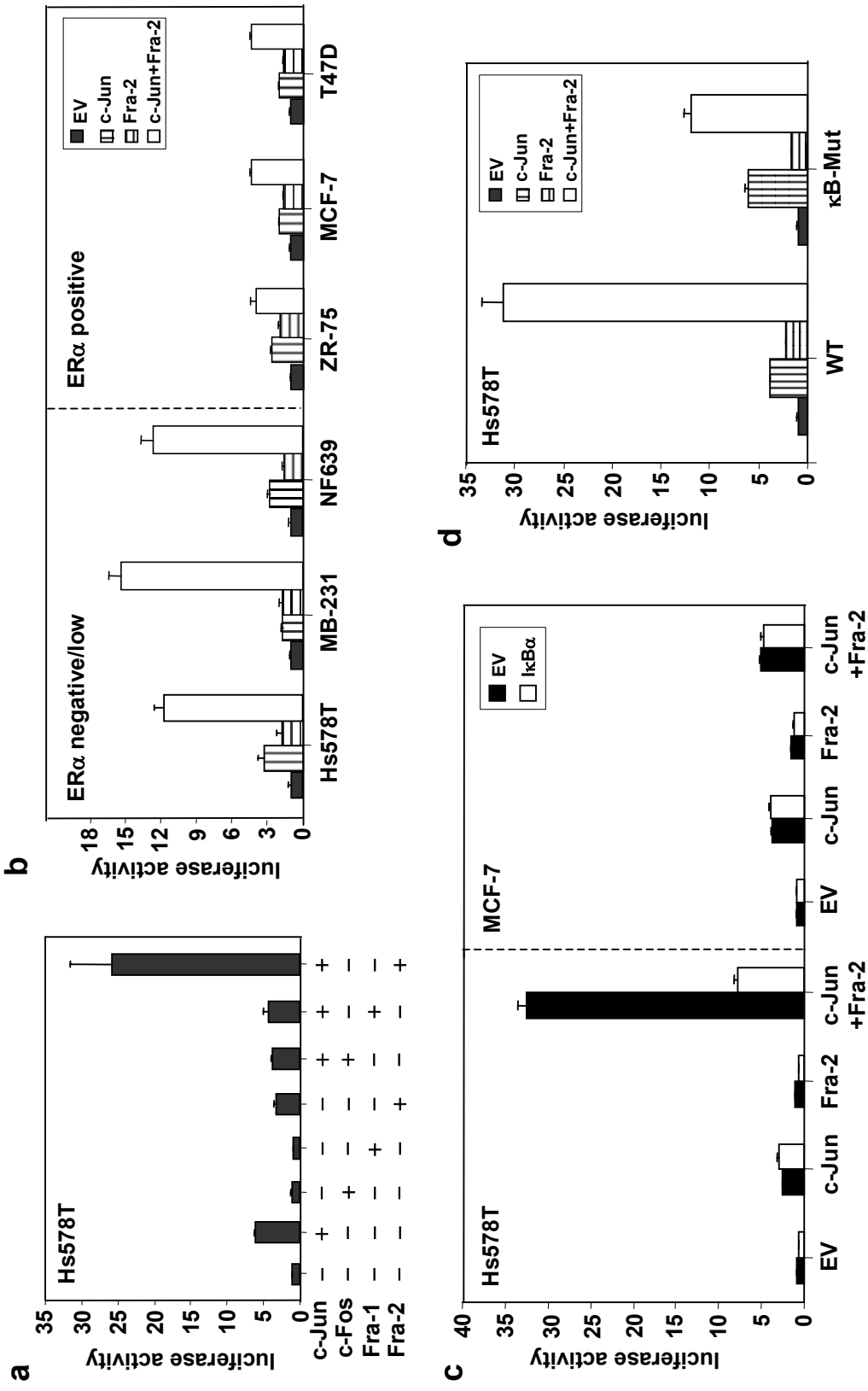
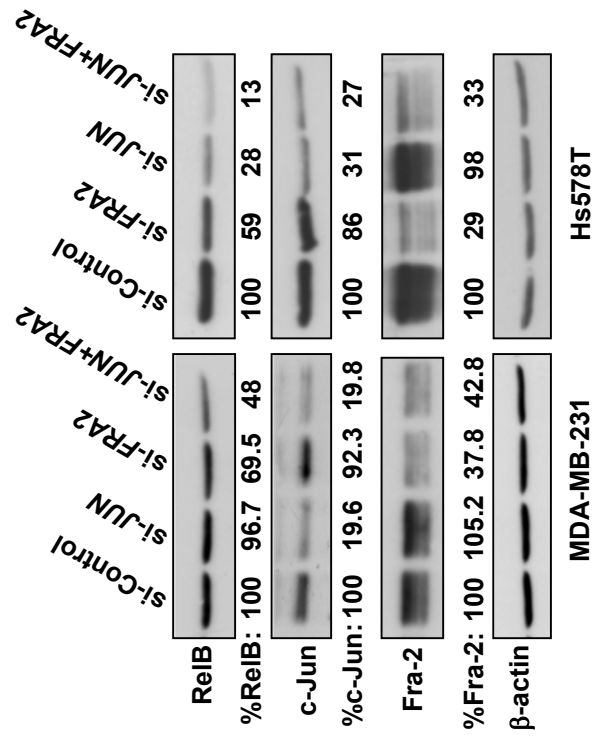


Fig. 2a-d, Wang et.al

e



f

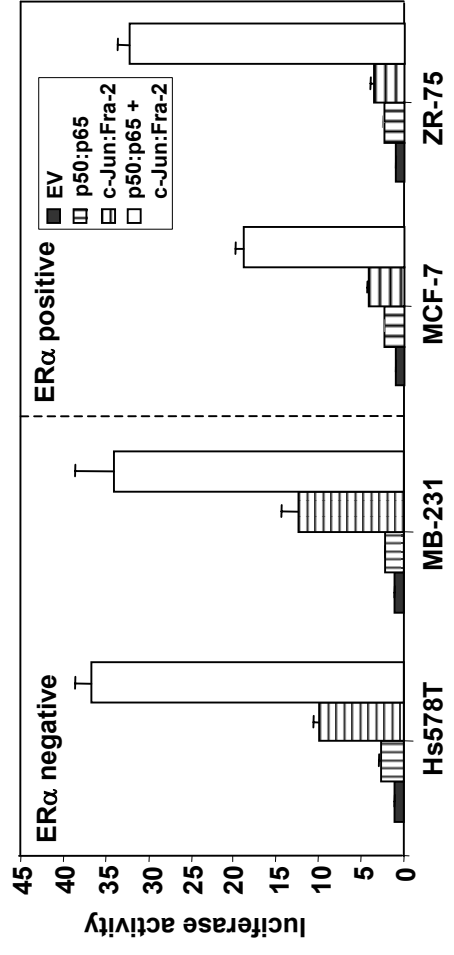


Fig. 2e-f, Wang et.al

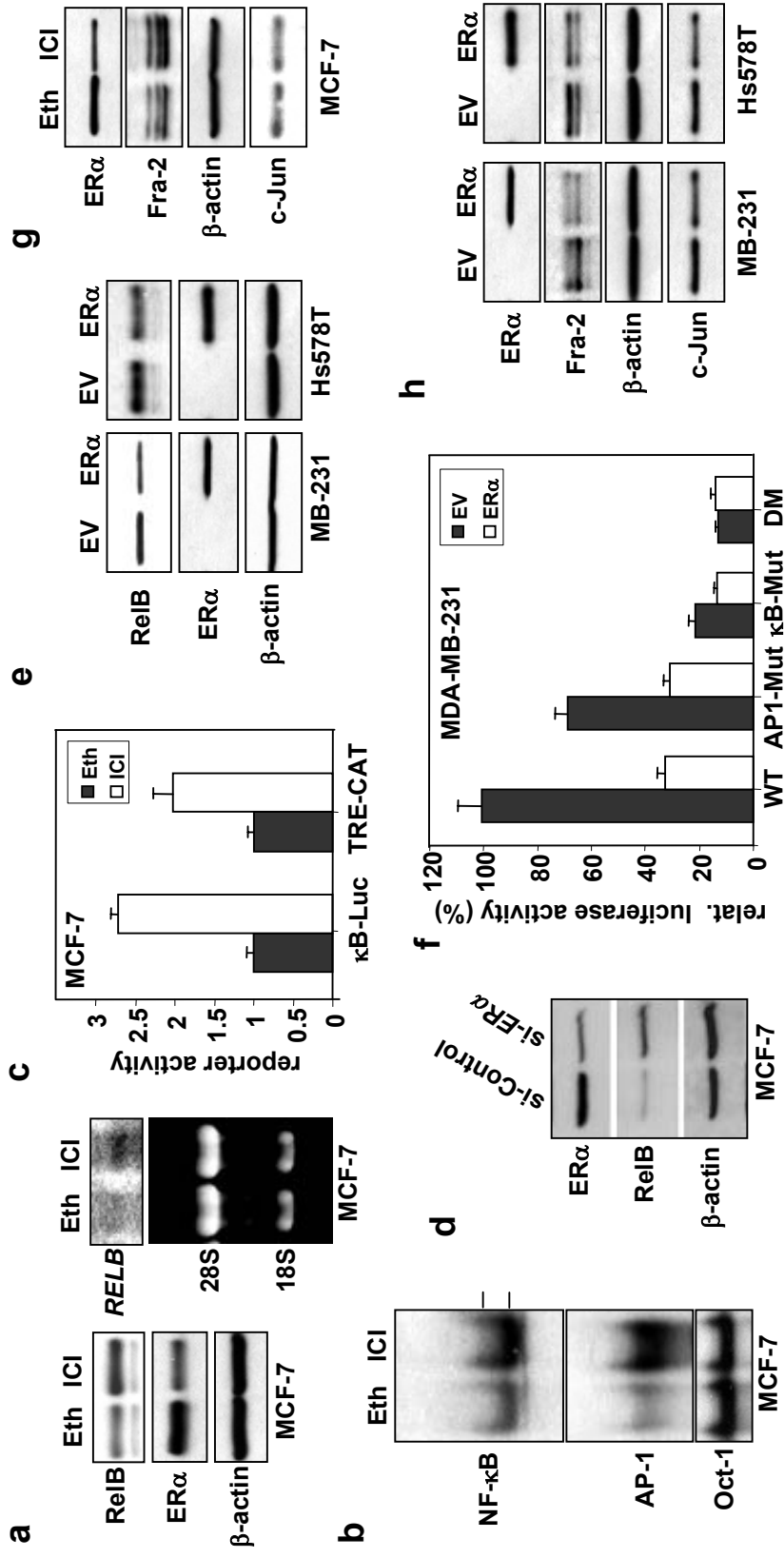


Fig. 3a-h, Wang et.al

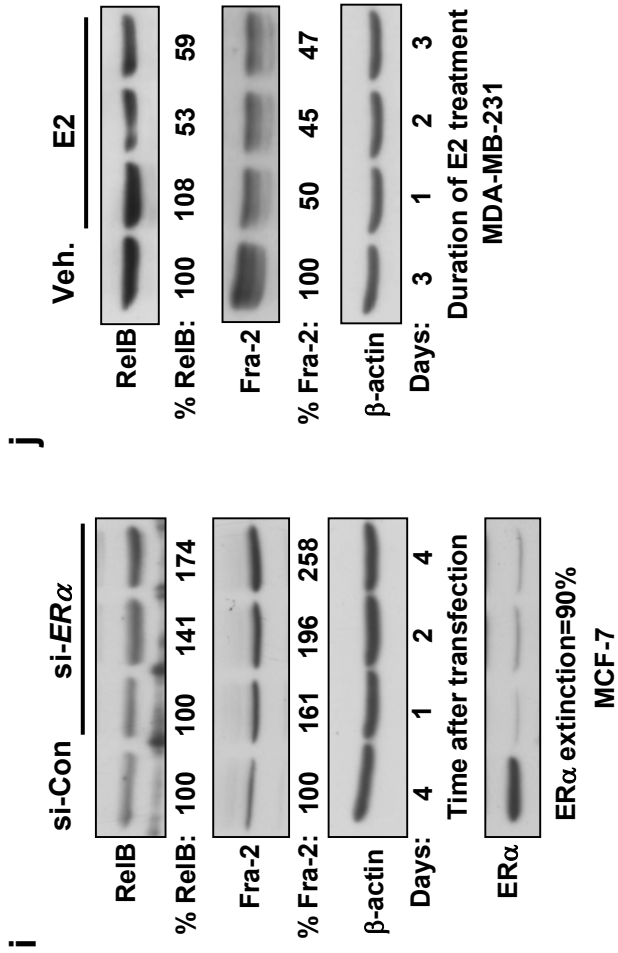


Fig. 3i-j, Wang et al.

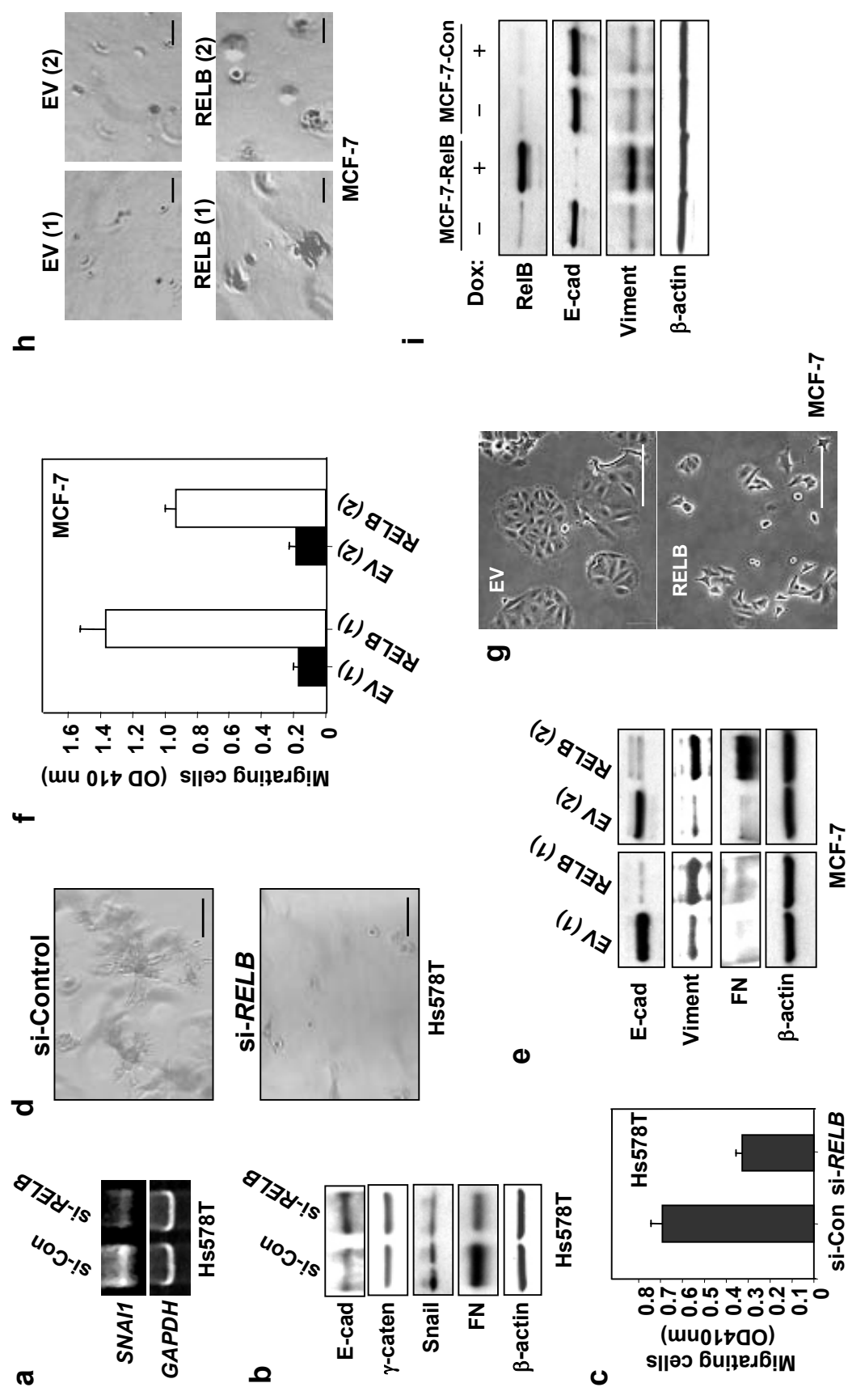


Fig. 4, Wang et.al

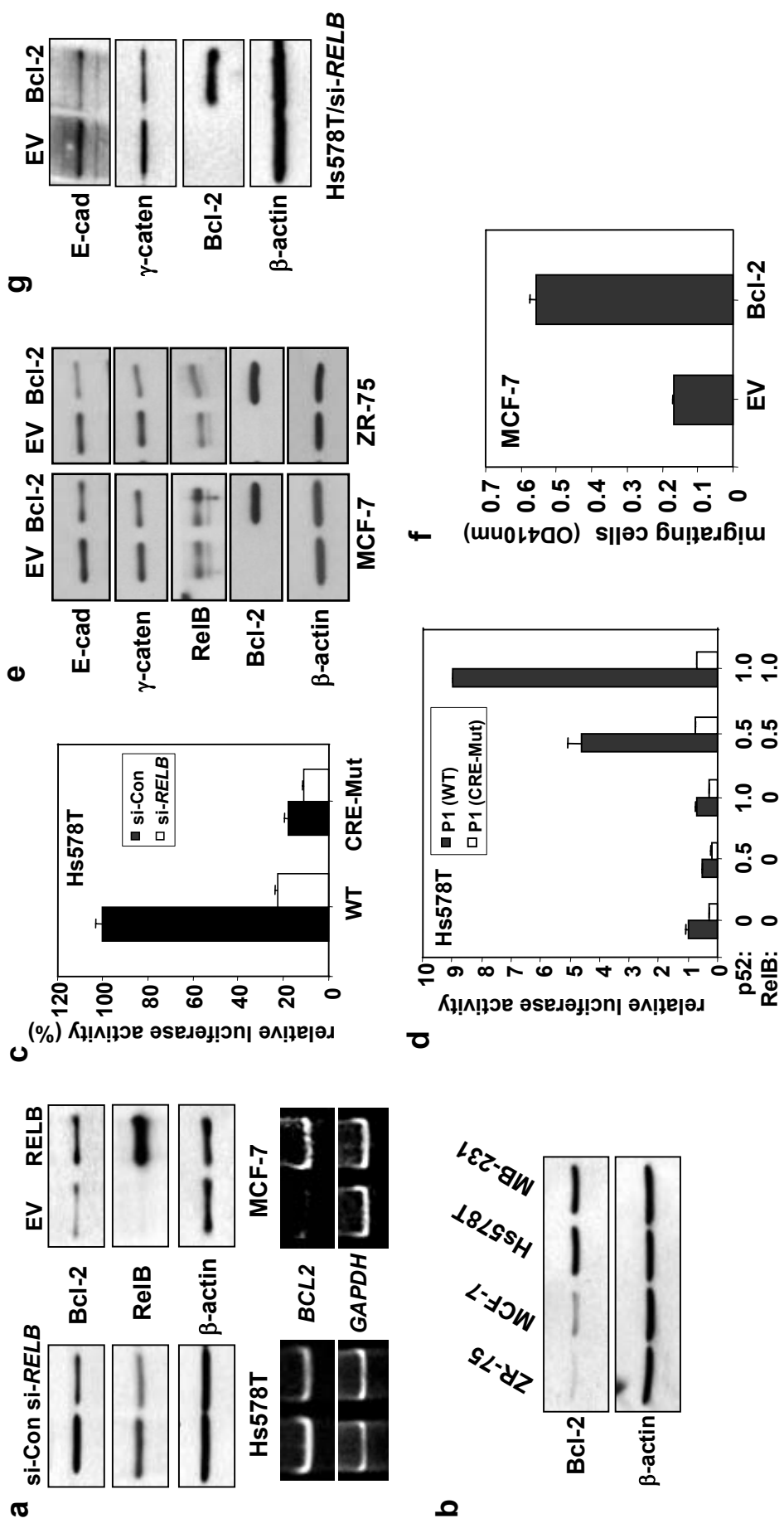


Fig. 5a-g, Wang et al.

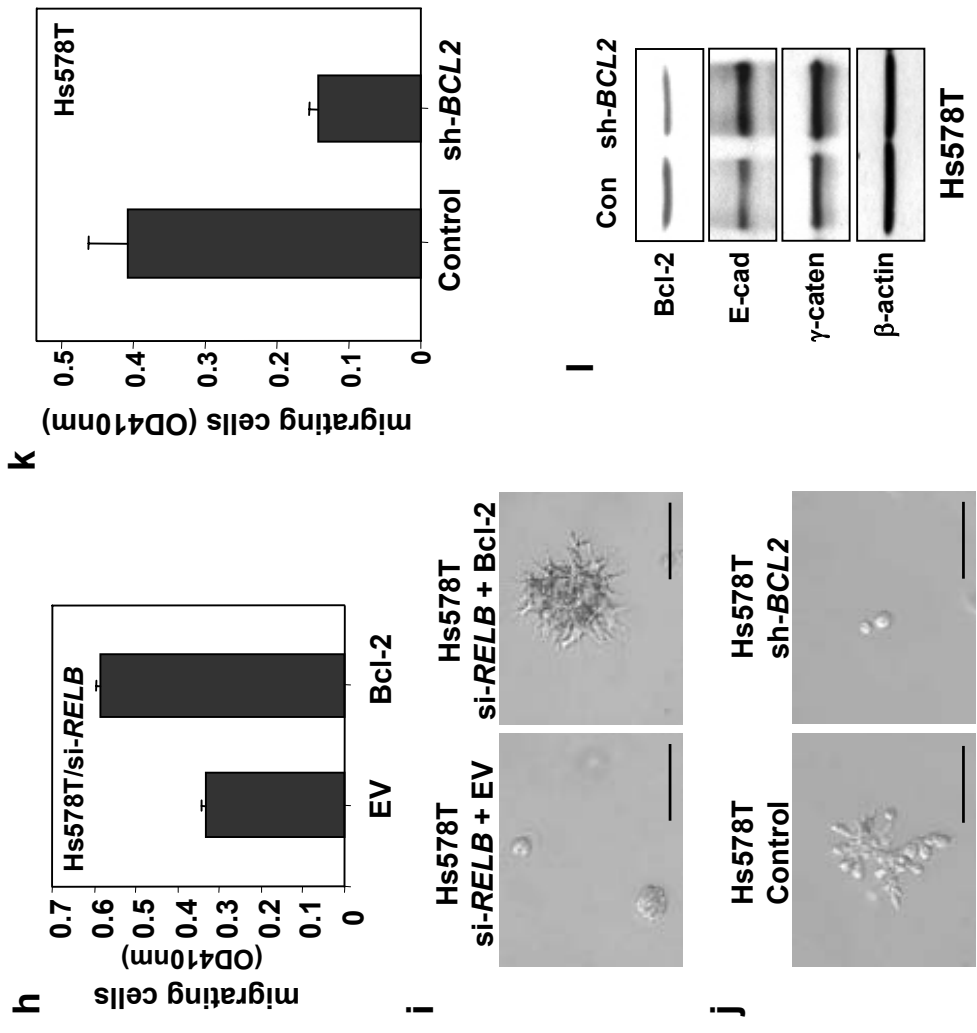


Fig. 5h-l, Wang et al.

Supplementary Data

Figure S1 ER α represses *de novo* synthesis of RelB. (a1) T47D cells were treated with 1 μ M ICI 182,780 (ICI) or equivalent volume of vehicle ethanol (Eth) for 48 h and WCEs (25 μ g) analyzed by immunoblotting for RelB, ER α , and β -actin. RelB levels normalized to β -actin in cells treated with ICI 182,780 are presented relative to cells treated with control ethanol. (a2) T47D cells were treated as above and mRNA (20 μ g) subjected to Northern blot analysis using human *RELB* cDNA as probe. Ethidium bromide staining of the gel confirmed equal loading. (a3) T47D cells were treated as above, and nuclear extracts (5 μ g) subjected to EMSA using oligonucleotides containing either NF- κ B, AP-1 or Oct-1 elements, as probes. (a4) T47D cells were transiently transfected, in triplicate, with 0.5 μ g NF- κ B or AP-1 element driven constructs κ B-Luc or TRE-CAT, respectively and 0.5 μ g SV40- β -gal. Post-transfection (6 h), cells were treated with 1 μ M ICI 182,780 or equivalent volume of vehicle ethanol for 40 h. Luciferase and CAT activities were determined and values normalized by β -gal activity presented as the mean \pm S.D. from three separate experiments (with the control ethanol sample set to 1). (b) Stable Hs578T transfectants expressing either sense *RELB* (si-Con) or siRNA *RELB* (si-*RELB*) were prepared. (b1) RNA (20 μ g) was subjected to Northern blot analysis using human *RELB* cDNA as probe. Ethidium bromide staining of the gel confirmed equal loading. (b2) Nuclear extracts (25 μ g) were analyzed by immunoblotting for levels of RelB, p65 and Lamin B, as loading control. (c) WCEs were prepared from MDA-MB-231 cells transiently expressing sense *RELB* (si-Con) or siRNA *RELB* (si-*RELB*). Samples (50 μ g) were analyzed by immunoblotting for E-cadherin, γ -catenin (γ -caten), Snail, fibronectin (FN), β -actin, and RelB.

Figure S2 RelB expression promotes mesenchymal phenotype via induction of Bcl-2. (a) Stable MCF-7 clones expressing either RELB or EV DNA were isolated: RELB(1), RELB(2), EV(1), and EV(2). Cells were transiently transfected, in triplicate, with 0.5 μ g κ B-Luc vector, and 0.5 μ g SV40- β -gal. Post-transfection (48 h), luciferase and β -gal activities were determined and normalized values presented relative to EV transfection, which was set at 1 (mean \pm S.D from three separate experiments). Inset: nuclear extracts (25 μ g) from the cells, indicated below, were subjected to immunoblot analysis for RelB, p65, and Lamin B. (b) WCEs (25 μ g) from MCF-7 RELB and control cells were analyzed by immunoblotting for cyclin D1, product of an NF- κ B target gene, and for β -actin. (c) ZR-75 cells were transiently transfected, in triplicate, with 1.0 μ g WT or CRE-Mutant P1 *BCL2* promoter-Luc vector, the indicated dose of p52 or RelB expression vectors, 0.5 μ g SV40- β -gal and empty vector pcDNA3 (EV) to make a total of 3.5 μ g DNA. Post-transfection (48 h), luciferase and β -gal activities were determined and normalized luciferase activities presented (mean \pm S.D. from three separate experiments).

Figure S3 RelB reduces E-cadherin expression in MCF-7 cells. The levels of E-cadherin in stable MCF-7 RELB and control cells were determined by indirect immunofluorescence microscopy using mouse anti-E-cadherin (primary) and Alexa594 anti-mouse (secondary) antibodies. Nuclei were stained with DAPI. Fluorescence microscopy was performed using a Zeiss Axiovert 200M microscope. Individual and merged images are shown. Scale bar, 100 μ m.

Figure S4 Bcl-2 reduces E-cadherin expression in MCF-7 cells. The levels of E-cadherin in MCF-7 stable cells with either EV or full length Bcl-2 DNA were determined by indirect

immunofluorescence microscopy using mouse anti-E-cadherin (primary) and Alexa594 anti-mouse (secondary) antibodies, as in Figure S3. Scale bar, 100 μm .

Figure S5 Full scans of original Western blots and EMSA gel. (a) Full scans of immunoblots of ER α and RelB in Figure 1a top panel. ns, nonspecific band. (b) Full scans of AP-1 and NF- κ B EMSA in Figure 1e. (c) Full scan of E-cadherin immunoblot in Figure 4i.

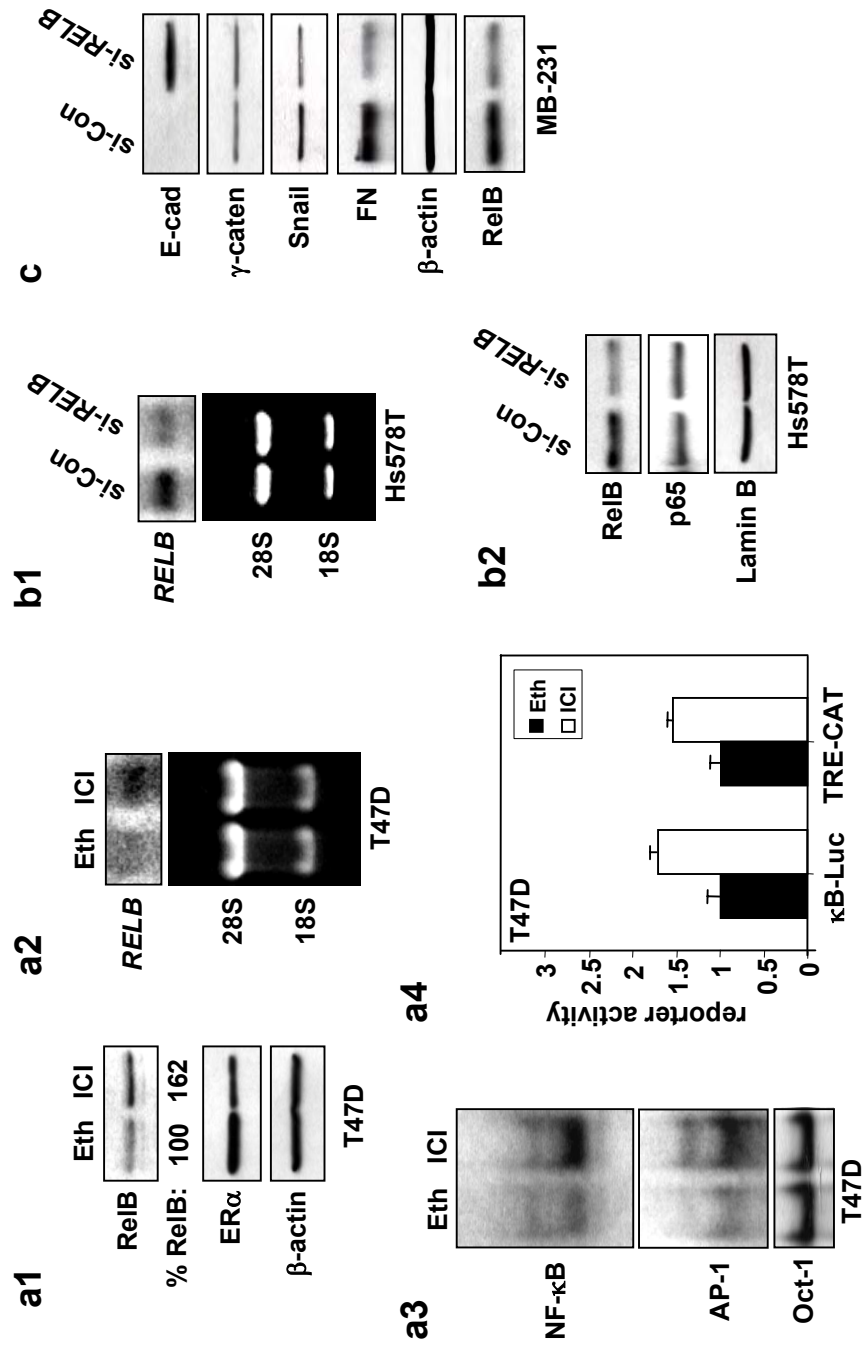


Fig S1. Wang et al.,

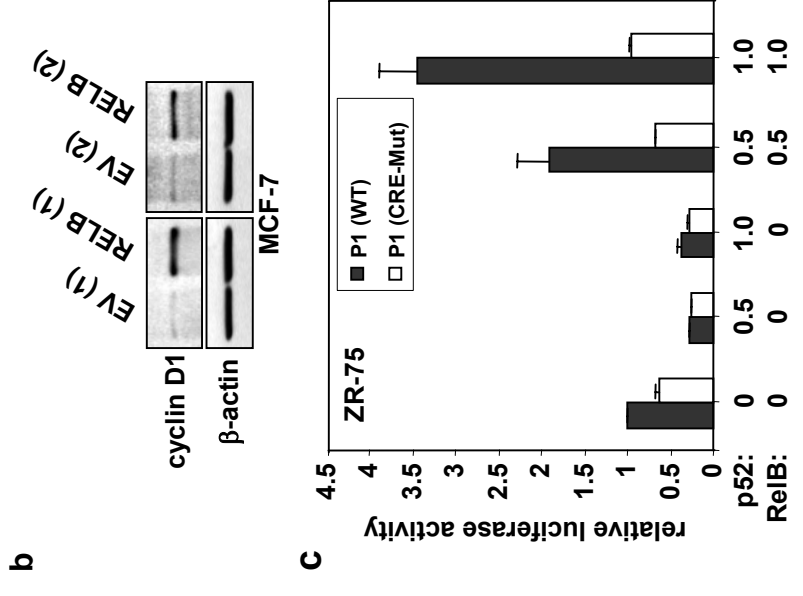
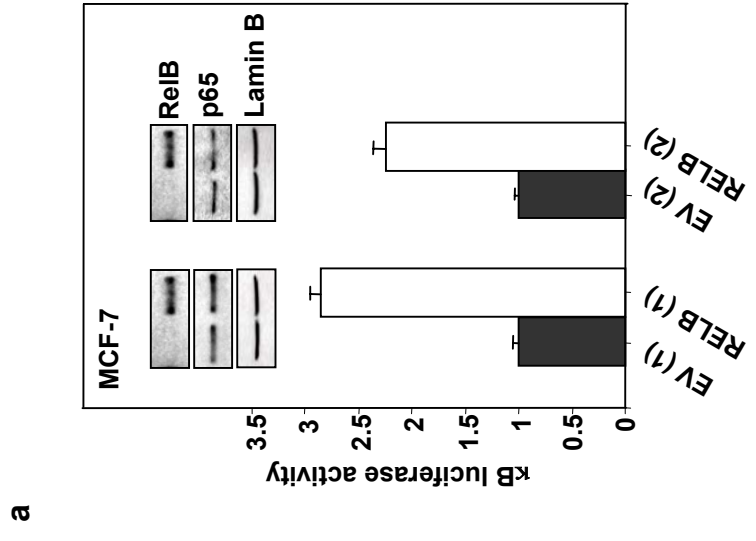


Fig S2. Wang et al.,

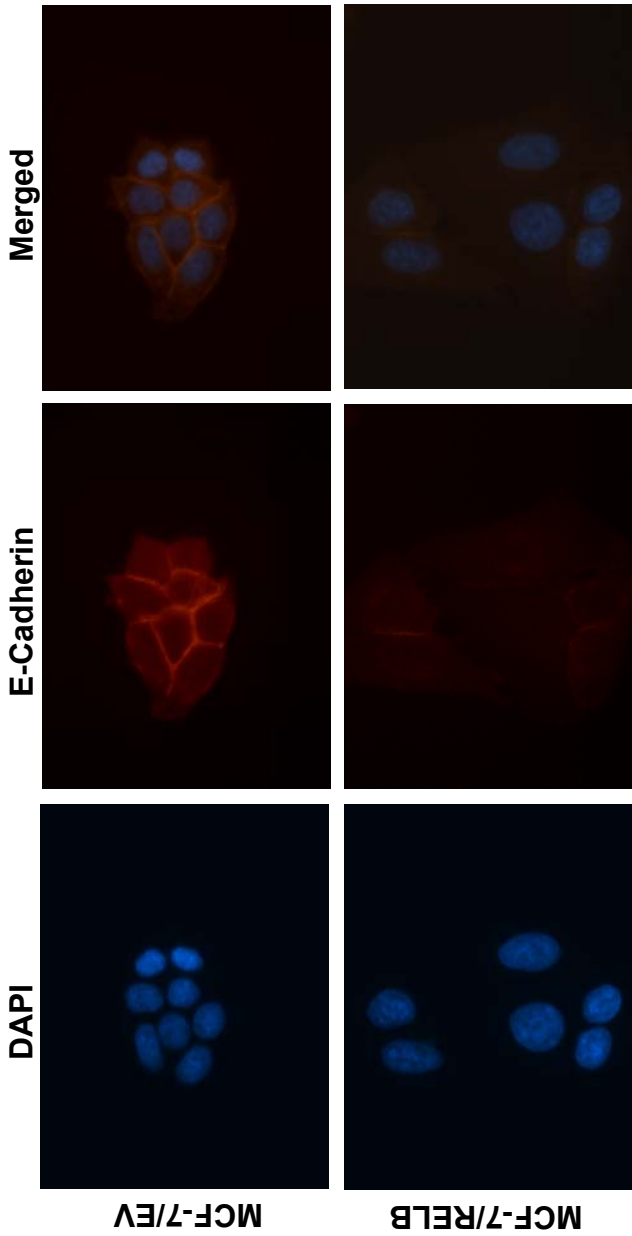


Fig. S3, Wang et al.,

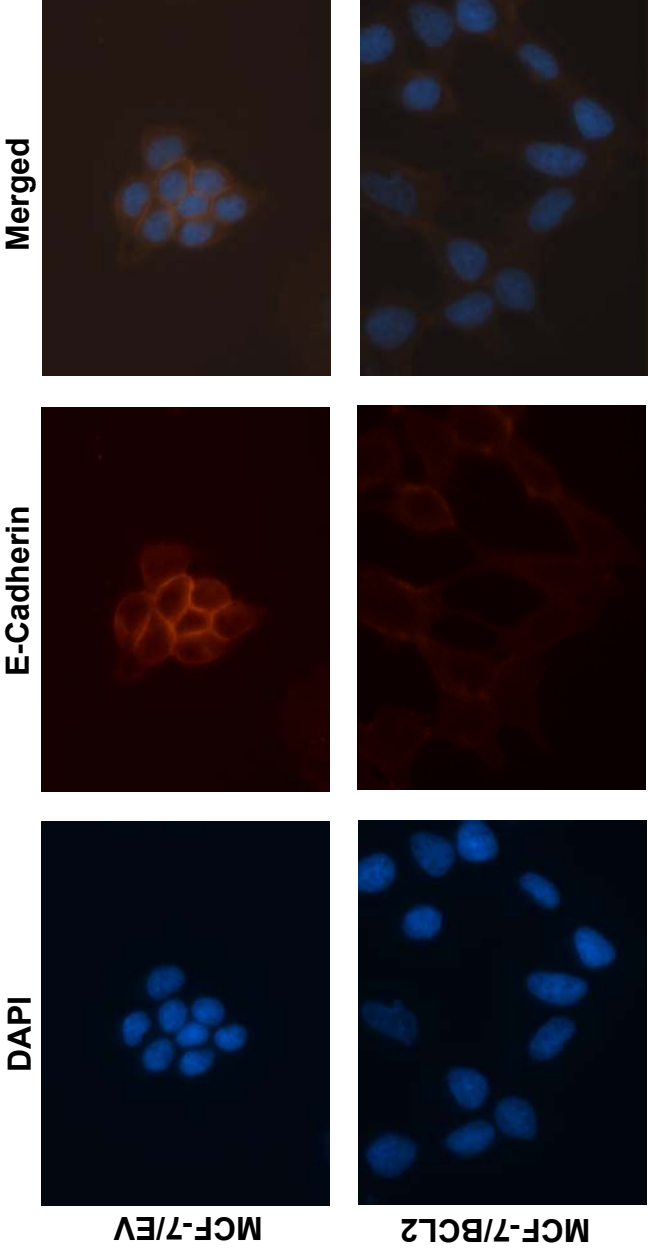


Fig. S4, Wang et al.,

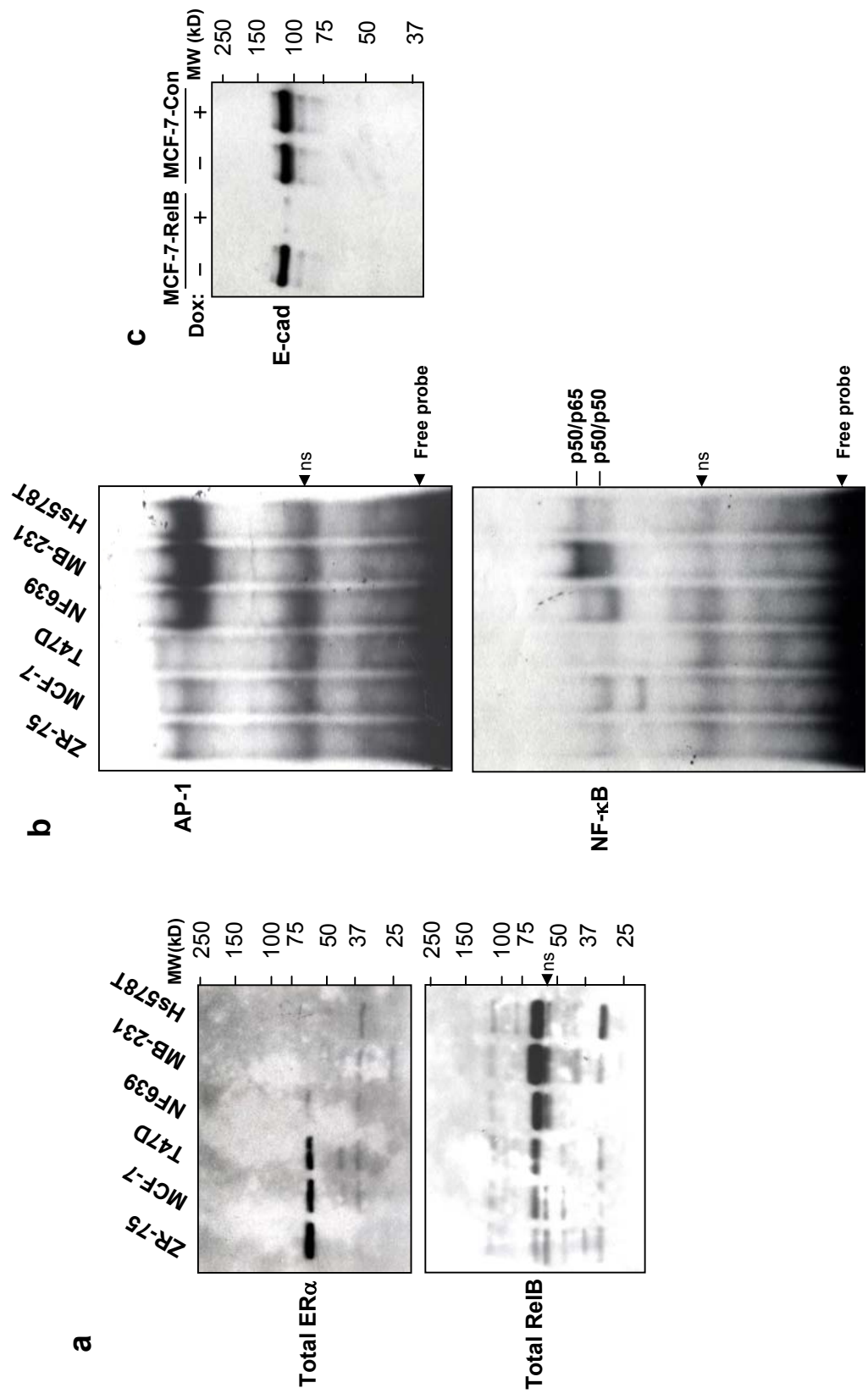


Fig. S5, Wang et al.